

3-D linearized scattering of surface waves and a formalism for surface wave holography

Roel Snieder *Department of Theoretical Geophysics, University of Utrecht, Budapestlaan 4, PO Box 80.021, 3508 TA Utrecht, The Netherlands*

Accepted 1985 August 6. Received 1985 August 6; in original form 1985 May 6

Summary. Scattering of surface waves by lateral heterogeneities is analysed in the Born approximation. It is assumed that the background medium is either laterally homogeneous, or smoothly varying in the horizontal direction. A dyadic representation of the Green's function simplifies the theory tremendously. Several examples of the theory are presented. The scattering and mode conversion coefficients are shown for scattering of surface waves by the root of an Alpine-like crustal structure. Furthermore a 'great circle theorem' in a plane geometry is derived. A new proof of Snell's law is given for surface wave scattering by a quarter-space. It is shown how a stationary phase approximation can be used to simplify the Fourier synthesis of the scattered wave in the time domain. Finally a procedure is suggested to do 'surface wave holography'.

Key words: Born, inversion, scattering, seismology, surface waves

1 Introduction

The propagation of surface waves in a laterally homogeneous medium is nowadays well understood (Aki & Richards 1980). Unfortunately there is no exact theory yet for the propagation of surface waves in a three-dimensional laterally varying medium. It is desirable to have such a theory because there are several observations indicating that short-period (< 20 s) surface waves are distorted severely by the lateral heterogeneities in the Earth. Levshin & Berteussen (1979) and Bungum & Capon (1974) give evidence of the scattering of short-period surface waves by lateral inhomogeneities.

The classical approach used in the analysis of surface waves in a laterally inhomogeneous earth is to assume that the surface waves are only influenced by the heterogeneities on the great circle joining the source and the receiver. A theoretical justification for this assumption is given for weak and smooth heterogeneities by Backus (1964), Jordan (1978) or Dahlen (1979). However, the observations of Levshin & Berteussen (1979) and Bungum & Capon (1974) show that in some cases an appreciable fraction of the surface wave energy propagates over non-great circle paths.

The effect of lateral heterogeneities on surface wave propagation in two dimensions has

received considerable interest. Knopoff & Hudson (1964) investigated the transmission of Love waves through a continental margin using a representation theorem. They modelled the continental margin by a vertical interface between two media. Alsop (1966) and Malichewsky (1979) studied the same model by minimizing the stress mismatch or the energy flux mismatch across the continental margin. However, none of these models could handle a non-zero angle of incidence, so that conversions from Love waves to Rayleigh waves could not be described. Hudson (1977a) treated the effect of a heterogeneous strip by using a variational method. All these studies involved some form of approximation. Finally, Kennett (1984a) devised an exact theory for the propagation of surface waves in a 2-D laterally heterogeneous medium.

The 3-D surface wave problem has received considerably less attention. Gregersen & Alsop (1974) and Alsop, Goodman & Gregersen (1974) considered the reflection and the transmission of surface waves in three dimensions by a vertical discontinuity. They did this by decomposing the surface wave in homogeneous and inhomogeneous body waves and using expressions for the reflection and transmission by an infinite discontinuity. However, their solutions did not satisfy the boundary conditions at the surface, so that it is not clear how useful their results are. Recently Its & Yanovskaya (1985) studied the 3-D reflection and transmission of surface waves at a vertical or weakly tilted discontinuity in a more rigorous way.

For 3-D media with a smooth lateral heterogeneity, ray tracing (Babich, Chikhachev & Yamovskaya 1976) or Gaussian beams (Yomogida & Aki 1985) are suitable techniques to describe the propagation of surface waves. However, it is impossible to treat sharp horizontal heterogeneities with these methods. Therefore, the theory for surface wave propagation in 3-D laterally heterogeneous media was restricted to lateral smoothly varying media, and to media consisting of two welded quarter-spaces. This was not very satisfactory since one would like to describe the scattering effects of an arbitrary distribution of scatterers in three dimensions.

The Born approximation is very useful in incorporating these effects. This approximation was first applied to the 2-D surface wave problem by Kennett (1972) who gave a derivation in wavenumber space. Subsequent papers used a similar theory to describe the scattering of body waves, see Hudson (1977b), Malin (1980), Malin & Phinney (1985) or Wu & Aki (1985). Herrera (1964) and Herrera & Mal (1965) used the Born approximation to describe 3-D surface wave scattering, and gave an expression for the scattered surface wave using representation theorems. Their results did not receive much attention because no convenient form of the Green's function was available. Therefore the Born approximation has not been used yet to describe surface wave scattering by organized 3-D heterogeneities. The aim of this paper is to provide such a scattering theory. The theory, as it is presented here, applies to scattering in the far field in a plane geometry.

In order to do this, a dyadic representation of the far field Green's function in a laterally homogeneous medium is presented in Section 2. The representation is similar to the dyadic form of the Green's function derived by Ben-Menahem & Singh (1968) for a homogeneous sphere, but is much easier to interpret. The Green's function for an elastic half-space consists of a surface wave part and a body wave part. In this study the body wave contribution to the Green's function has been neglected throughout. The reason for this is that the theory relies heavily on a dyadic representation of the Green's function. Unfortunately, there is no dyadic representation of the body wave Green's function in a layered medium available. This problem can be overcome in two ways. One alternative is to use a locked mode approximation (Harvey 1981). Another option is to consider an elastic sphere instead of an elastic half-space. In that case both surface waves and body waves can be expressed in normal

modes. The generalization of the theory presented in this paper to a laterally inhomogeneous sphere is presented in Snieder & Nolet (in preparation).

In Sections 3 and 4 the dyadic representation of the surface wave Green's function is used to derive the Born approximation for surface waves in the far field. The theory describes mode conversion in a natural way because the Green's function is a superposition of all surface wave modes. In Section 5 this theory is generalized for the important application of a background medium with smooth lateral variations.

The second half of the paper deals with some examples and illustrations of the theory. These examples by no means exhaust the possibilities of the theory. In Section 6 the interaction terms and the radiation patterns are presented for surface wave scattering by a point scatterer which has a vertical structure similar to the root of the Alps.

The advantage of the formulation using a dyadic representation of the Green's function is that the final expression for the scattered wave is quite simple. This enables one to use the formalism for the scattering of surface waves in realistic situations. Section 7 features two examples of this. Propagation through a band-like structure is discussed. This leads to a 'great circle theorem' in a flat geometry. Furthermore the reflection by a quarter-space is treated as a simple example of scattering by a continental margin.

All the derivations are given in the frequency domain, since surface waves are dispersive. In Section 8 it is shown how a stationary phase approximation leads to an efficient formulation in the time domain, which is useful for calculating synthetic seismograms.

One would like to use scattered surface waves to invert for the location and the structure of the scatterers. This can in principle be done with an inversion scheme similar to the algorithm of Tarantola (1984a, b). It is shown in Section 9 how 'back propagation' of scattered surface waves can be used to invert for the scatterers.

In this paper the summation convention is used unless stated otherwise. Latin indices are used to denote vector components, while Greek indices are used for the mode numbers. The dot product which is used is defined by:

$$[p \cdot q] = p_i^* q_i \quad (1)$$

where * denotes complex conjugation. Double contractions are defined by:

$$[A : B] = A_{ij}^* B_{ji}. \quad (2)$$

Finally, in order to see the limitations of the theory the assumptions which are used throughout the paper are listed. It is assumed that:

- there is a plane geometry;
- the interaction with body waves can be neglected;
- the far field approximation can be used;
- the heterogeneity is weak;
- the scatterers are buried.

2 The dyadic representation of the far field Green's function of a laterally homogeneous medium

The surface wave Green's function in the spectral domain for the excitation of a laterally homogeneous elastic medium with density ρ and elastic parameters λ and μ by a point force is given by Aki & Richards (1980, chapter 7). The Green's function contains a matrix, but this matrix can be rewritten as a dyad. The expressions of Aki & Richards include an azimuth angle φ , which depends on the positions of the source and the receiver. This

azimuth dependence can be interpreted easily by rewriting the Green's function in a dyadic form. Both for Love waves and for Rayleigh waves the far field Green's function can be written as:

$$G_{ij}(\mathbf{r}, \mathbf{r}_s) = p_i^\nu(z, \varphi) p_j^{\nu*}(z_s, \varphi) \frac{\exp [i(k_\nu X + \pi/4)]}{\sqrt{(\pi/2)k_\nu X}}. \quad (3)$$

For Love waves \mathbf{p}^ν is given by:

$$\mathbf{p}^\nu(z, \varphi) = \begin{pmatrix} -l_1^\nu(z) \sin \varphi \\ l_1^\nu(z) \cos \varphi \\ 0 \end{pmatrix} \quad (4a)$$

while for Rayleigh waves:

$$\mathbf{p}^\nu(z, \varphi) = \begin{pmatrix} r_1^\nu(z) \cos \varphi \\ r_1^\nu(z) \sin \varphi \\ ir_2^\nu(z) \end{pmatrix}. \quad (4b)$$

\mathbf{p}^ν is called the polarization vector. The index ν refers to the mode number; it should be remembered that modal summation is implied in (3). The functions $l_1^\nu(z)$, $r_1^\nu(z)$ and $r_2^\nu(z)$ are the surface wave eigenfunctions in the notation of Aki & Richards. It is assumed that the eigenfunctions are normalized in such a way that:

$$8c_\nu U_\nu I_1^\nu = 1 \text{ (no summation)}. \quad (5)$$

Here c_ν and U_ν are the phase velocity and the group velocity of mode ν . The integral I_1^ν is for Love waves defined by:

$$I_1^\nu = \frac{1}{2} \int \rho(z) l_1^{\nu 2}(z) dz \quad (6a)$$

and for Rayleigh waves:

$$I_1^\nu = \frac{1}{2} \int \rho(z) (r_1^{\nu 2}(z) + r_2^{\nu 2}(z)) dz. \quad (6b)$$

The polarization vectors can be interpreted by expressing them in the following vector form:

$$\mathbf{p}^\nu(z, \varphi) = l_1^\nu(z) \hat{\varphi} \quad \text{for Love waves} \quad (7)$$

$$\mathbf{p}^\nu(z, \varphi) = r_1^\nu(z) \hat{\Delta} + ir_2^\nu(z) \hat{z} \quad \text{for Rayleigh waves.} \quad (8)$$

(See Fig. 1 for the definition of $\hat{\Delta}$ and $\hat{\varphi}$.) It can now be understood why the \mathbf{p} vectors are called the polarization vectors, since they describe the direction in which the displacement vector oscillates. In the far field, this oscillation is purely transverse for Love waves, while Rayleigh waves oscillate both in the radial and vertical direction.

From this point on, Love and Rayleigh waves are treated in a unified way, and the modal summation involves both Love and Rayleigh waves. Using the representation (3), the displacement excited by a point force \mathbf{F} oscillating with angular frequency ω can be written as:

$$\mathbf{u}^0(\mathbf{r}) = \mathbf{p}^\nu(z, \varphi) \frac{\exp [i(k_\nu X + \pi/4)]}{\sqrt{(\pi/2)k_\nu X}} [\mathbf{p}^\nu(z_s, \varphi) \cdot \mathbf{F}]. \quad (9)$$

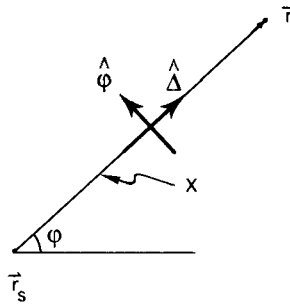


Figure 1. Geometry for the direct wave in a laterally homogeneous medium.

It can be seen explicitly that the displacement oscillations are in the \mathbf{p}^ν direction. The excitation is described by the dot product in the right side of (9). This means that only the projection of the force on the polarization vector contributes to the excitation.

In subsequent sections the gradient of the Green's function is needed. The gradient is derived here in the far field limit, since the Green's function itself is already in the far field limit. The azimuthal derivative in the gradient can be neglected, since it is $O(1/kX)$ compared to the radial derivative. The gradient with respect to the receiver position (index 1), or the source position (index 2) is in the far field limit:

$$\tilde{\nabla}_1 G_{ij}(\mathbf{r}_1, \mathbf{r}_2) = ik_\nu \hat{\Delta} p_i^\nu(z_1, \varphi) p_j^{\nu*}(z_2, \varphi) \frac{\exp [i(k_\nu X + \pi/4)]}{\sqrt{(\pi/2)k_\nu X}} \quad (10a)$$

$$\tilde{\nabla}_2 G_{ij}(\mathbf{r}_1, \mathbf{r}_2) = -ik_\nu \hat{\Delta} p_i^\nu(z_1, \varphi) p_j^{\nu*}(z_2, \varphi) \frac{\exp [i(k_\nu X + \pi/4)]}{\sqrt{(\pi/2)k_\nu X}} \quad (10b)$$

$$\partial_{z_1} G_{ij}(\mathbf{r}_1, \mathbf{r}_2) = (\partial_{z_1} p_i^\nu(z_1, \varphi)) p_j^{\nu*}(z_2, \varphi) \frac{\exp [i(k_\nu X + \pi/4)]}{\sqrt{(\pi/2)k_\nu X}} \quad (10c)$$

$$\partial_{z_2} G_{ij}(\mathbf{r}_1, \mathbf{r}_2) = p_i^\nu(z_1, \varphi) (\partial_{z_2} p_j^{\nu*}(z_2, \varphi)) \frac{\exp [i(k_\nu X + \pi/4)]}{\sqrt{(\pi/2)k_\nu X}} \quad (10d)$$

In these expressions $\tilde{\nabla}$ is the horizontal gradient operator.

With these expressions the excitation by a moment tensor can be determined. The response to a single couple follows by superposing the response to point force \mathbf{F} at $\mathbf{r}_s + \delta$ to the response to a point force $-\mathbf{F}$ at $\mathbf{r}_s - \delta$. The response to this single couple follows by Taylor expanding the superposition in δ , and using (10a–d) for the gradient. Interchanging the direction of \mathbf{F} and δ and adding the single couple displacement fields leads to the following response to the excitation by a moment tensor:

$$\mathbf{u}^0(\mathbf{r}) = \mathbf{p}^\nu(z, \varphi) \frac{\exp [i(k_\nu X + \pi/4)]}{\sqrt{(\pi/2)k_\nu X}} [(ik_\nu \hat{\Delta} + \hat{z} \partial_{z_s}) \mathbf{p}^\nu(z_s, \varphi) : M] \quad (11)$$

where M is defined as:

$$M = 2(\delta \mathbf{F} + \mathbf{F} \delta). \quad (12)$$

Note that the factor $-i$ coming from the horizontal gradient in the source coordinate is absorbed in the definition of the dot product.

All the following sections deal with the excitation by a point force, but the results can be

generalized everywhere in case of excitation by a double couple by making the following substitution:

$$[\mathbf{p}^v(z_s, \varphi) \cdot \mathbf{F}] \rightarrow [(ik_v \hat{\Delta} + \hat{z} \partial_{z_s}) \mathbf{p}^v(z_s, \varphi) : M]. \quad (13)$$

3 The Born approximation

The effect of lateral heterogeneities is treated here in a linearized way by using the Born approximation for the scattered wave. Suppose that the structural parameters in the medium can be written in the following way:

$$\mu(x, y, z) = \mu_0(z) + \epsilon \Delta\mu(x, y, z) \quad (14a)$$

$$\lambda(x, y, z) = \lambda_0(z) + \epsilon \Delta\lambda(x, y, z) \quad (14b)$$

$$\rho(x, y, z) = \rho_0(z) + \epsilon \Delta\rho(x, y, z). \quad (14c)$$

The parameters μ_0 , λ_0 and ρ_0 define a laterally homogeneous background medium, which has a Green's function as presented in the last section. The parameter ϵ has been added to indicate that the inhomogeneity is weak, and serves only for bookkeeping purposes.

The equations of motion of the laterally heterogeneous system can be written as:

$$L_{ij}u_j = F_i \quad (15)$$

with

$$L_{ij} = -\delta_{ij}\rho\omega^2 - \partial_i\lambda\partial_j - \partial_j\mu\partial_i - \delta_{ij}\partial_k\mu\partial_k. \quad (16)$$

This operator can be written in the form $L = L^0 + \epsilon L^1$ by inserting (14a–c) in (15). The displacement field can be expressed as a perturbation series: $\mathbf{u} = \mathbf{u}^0 + \epsilon\mathbf{u}^1 + O(\epsilon^2)$. If these expressions are inserted in (15), then the terms of zeroth order and first order in ϵ lead to the relations:

$$L^0 \mathbf{u}^0 = \mathbf{F} \quad (17)$$

$$L^0 \mathbf{u}^1 = -L^1 \mathbf{u}^0. \quad (18)$$

If we now assume that the heterogeneity does not affect the boundary conditions (which may be a very debatable assumption in realistic situations), then both (17) and (18) can be solved with the Green's function of the background medium. This leads to the following expression for the direct wave:

$$\mathbf{u}^0 = \mathbf{GF}. \quad (19)$$

While the scattered wave is given by:

$$\mathbf{u}^1 = -GL^1 \mathbf{u}^0 = -GL^1 \mathbf{GF}. \quad (20)$$

The operator products in (19) and (20) imply both summation over matrix elements as well as integration over space variables of the Green's function. For example, (19) is an abbreviated notation for:

$$u_i^0(\mathbf{r}) = \int d^3r' G_{ij}(\mathbf{r}, \mathbf{r}') F_j(\mathbf{r}'). \quad (21)$$

For the moment we shall only concern ourselves with excitation by a point force in \mathbf{r}_s and

scattering by a point heterogeneity in \mathbf{r}_0 :

$$\Delta\mu(\mathbf{r}) = \Delta\mu\delta(\mathbf{r} - \mathbf{r}_0) \quad (22a)$$

$$\Delta\lambda(\mathbf{r}) = \Delta\lambda\delta(\mathbf{r} - \mathbf{r}_0) \quad (22b)$$

$$\Delta\rho(\mathbf{r}) = \Delta\rho\delta(\mathbf{r} - \mathbf{r}_0) \quad (22c)$$

$$\mathbf{F}(\mathbf{r}) = \mathbf{F}\delta(\mathbf{r} - \mathbf{r}_s). \quad (22d)$$

Since the theory in this approximation is linear in the heterogeneity, as well as in the excitation, more general situations can be handled by integration over both the heterogeneity and the excitation.

The unperturbed direct wave has been discussed in Section 2. The scattered wave is explicitly:

$$u_i^1(\mathbf{r}) = - \int d^3r' G_{ij}(\mathbf{r}, \mathbf{r}') L_{jk}^1(\mathbf{r}') G_{kl}(\mathbf{r}', \mathbf{r}_s) F_l(\mathbf{r}_s). \quad (23)$$

where the heterogeneity operator is:

$$L_{ij}^1(\mathbf{r}') = -\Delta\rho\omega^2 \delta_{ij} \delta(\mathbf{r}' - \mathbf{r}_0) \quad (i)$$

$$-\Delta\lambda \partial'_i \delta(\mathbf{r}' - \mathbf{r}_0) \partial'_j \quad (ii)$$

$$-\Delta\mu \partial'_j \delta(\mathbf{r}' - \mathbf{r}_0) \partial'_i \quad (iii)$$

$$-\Delta\mu\delta_{ij} \partial'_k \delta(\mathbf{r}' - \mathbf{r}_0) \partial'_k. \quad (iv) \quad (24)$$

The differentiations are all with respect to the \mathbf{r}' coordinates. Note that the differentiations act both on the delta functions as well as on the Green's function at the right of L^1 . The differentiation of the delta functions can be removed with a partial integration. For instance, the contribution of term (ii) to (23) can be rewritten:

$$\begin{aligned} & - \int d^3r' G_{ij}(\mathbf{r}, \mathbf{r}') \partial'_j [\Delta\lambda \delta(\mathbf{r}' - \mathbf{r}_0) \partial'_k G_{kl}(\mathbf{r}', \mathbf{r}_s)] F_l \\ & = \int d^3r' [\partial'_j G_{ij}(\mathbf{r}, \mathbf{r}')] \Delta\lambda \delta(\mathbf{r}' - \mathbf{r}_0) [\partial'_k G_{kl}(\mathbf{r}', \mathbf{r}_s)] F_l \\ & = \Delta\lambda [\partial_j^0 G_{ij}(\mathbf{r}, \mathbf{r}_0)] [\partial_k^0 G_{kl}(\mathbf{r}_0, \mathbf{r}_s)] F_l. \end{aligned}$$

The partial integration leads to a surface integral, which is zero for buried scatterers. If partial integration is also applied to the terms (iii) and (iv) the scattered wave takes the following form:

$$\begin{aligned} u_i^1(\mathbf{r}) & = [\Delta\rho\omega^2 G_{ij}(\mathbf{r}, \mathbf{r}_0) G_{jl}(\mathbf{r}_0, \mathbf{r}_s)] \quad (i) \\ & - \Delta\lambda (\partial_j^0 G_{ij}(\mathbf{r}, \mathbf{r}_0)) (\partial_k^0 G_{kl}(\mathbf{r}_0, \mathbf{r}_s)) \quad (ii) \\ & - \Delta\mu (\partial_k^0 G_{ij}(\mathbf{r}, \mathbf{r}_0)) (\partial_j^0 G_{kl}(\mathbf{r}_0, \mathbf{r}_s)) \quad (iii) \\ & - \Delta\mu (\partial_k^0 G_{ij}(\mathbf{r}, \mathbf{r}_0)) (\partial_k^0 G_{jl}(\mathbf{r}_0, \mathbf{r}_s))] F_l(\mathbf{r}_s). \quad (iv) \quad (25) \end{aligned}$$

This expression is not easy to interpret because of all the gradient terms of the Green's function. However, the expression may be simplified considerably by using the dyadic form for the Green's function (3) and its gradient (10a-d). After some algebra it follows that in

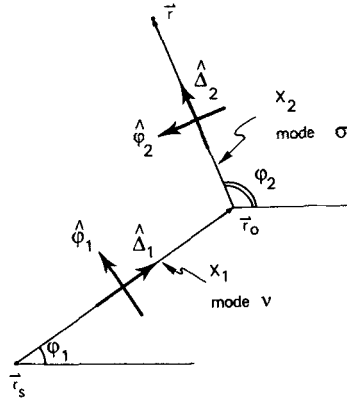


Figure 2. Geometry for the scattered wave in a laterally homogeneous background medium.

the notation of Fig. 2:

$$\mathbf{u}^1(\mathbf{r}) = \mathbf{p}^\sigma(z, \varphi_2) \frac{\exp [i(k_\sigma X_2 + \pi/4)]}{\sqrt{(\pi/2)k_\sigma X_2}} V^{\sigma\nu}(\mathbf{r}_0) \frac{\exp [i(k_\nu X_1 + \pi/4)]}{\sqrt{(\pi/2)k_\nu X_1}} [\mathbf{p}^\nu(z_s, \varphi_1) \cdot \mathbf{F}] \quad (26)$$

where $V^{\sigma\nu}$ is given by:

$$\begin{aligned} V^{\sigma\nu}(\mathbf{r}_0) &= \Delta\rho\omega^2 [\mathbf{p}^\sigma(z_0, \varphi_2) \cdot \mathbf{p}^\nu(z_0, \varphi_1)] & (i) \\ &- \Delta\lambda \{ (-ik_\sigma [\mathbf{p}^\sigma(z_0, \varphi_2) \cdot \hat{\Delta}_2] + [\partial_{z_0} \mathbf{p}^\sigma(z_0, \varphi_2) \cdot \hat{z}]) (ik_\nu [\hat{\Delta}_1 \cdot \mathbf{p}^\nu(z_0, \varphi_1)] \\ &\quad + [\hat{z} \cdot \partial_{z_0} \mathbf{p}^\nu(z_0, \varphi_1)]) \} & (ii) \\ &- \Delta\mu \{ [k_\sigma k_\nu [\mathbf{p}^\sigma(z_0, \varphi_2) \cdot \hat{\Delta}_1] [\hat{\Delta}_2 \cdot \mathbf{p}^\nu(z_0, \varphi_1)] \\ &\quad - ik_\sigma [\mathbf{p}^\sigma(z_0, \varphi_2) \cdot \hat{z}] [\hat{\Delta}_2 \cdot \partial_{z_0} \mathbf{p}^\nu(z_0, \varphi_1)] \\ &\quad + ik_\nu [\partial_{z_0} \mathbf{p}^\sigma(z_0, \varphi_2) \cdot \hat{\Delta}_1] [\hat{z} \cdot \mathbf{p}^\nu(z_0, \varphi_1)] \\ &\quad + [\partial_{z_0} \mathbf{p}^\sigma(z_0, \varphi_2) \cdot \hat{z}] [\hat{z} \cdot \partial_{z_0} \mathbf{p}^\nu(z_0, \varphi_1)] \} & (iii) \\ &- \Delta\mu \{ [k_\sigma k_\nu [\hat{\Delta}_2 \cdot \hat{\Delta}_1] [\mathbf{p}^\sigma(z_0, \varphi_2) \cdot \mathbf{p}^\nu(z_0, \varphi_1)] \\ &\quad + [\partial_{z_0} \mathbf{p}^\sigma(z_0, \varphi_2) \cdot \partial_{z_0} \mathbf{p}^\nu(z_0, \varphi_1)] \}. & (iv) \end{aligned} \quad (27)$$

The expression for the scattered wave (26) is now easy to interpret. If one reads (26) from right to left one follows the 'life history' of the scattered wave. The point force excites mode ν . The surface wave then travels to the point of scattering \mathbf{r}_0 , the phase shift and the geometrical spreading are determined by the propagation term $\exp i(k_\nu X_1 + \pi/4)/\sqrt{(\pi/2)k_\nu X_1}$. Then the wave is scattered by the interaction matrix $V^{\sigma\nu}$. After the scattering, which may include mode conversion since the modes σ and ν can be different, the wave propagates to the receiver. The oscillation at the receiver is finally given by the polarization vector $\mathbf{p}^\sigma(z, \varphi_2)$. Note that (26) implies a summation over all the surface wave modes, and that all the modes in principle interact with each other.

4 Analysis of the interaction matrix

The interaction matrix as given in (27) is very general, but is hard to interpret. However, (27) can be simplified by inserting the expressions (7) and (8) for the polarization vectors of

Love and Rayleigh waves. It turns out that even though the polarization vectors depend on the azimuthal angles φ_1 and φ_2 separately, the interaction matrix depends only on the scattering angle:

$$\varphi = \varphi_2 - \varphi_1. \quad (28)$$

As an example this is shown for the scattering of Love waves by the density variation:

$$V_{LL}^{\sigma\nu}(\mathbf{i}) = \Delta\rho\omega^2 l_1^\sigma(z_0)l_1^\nu(z_0)[\hat{\varphi}_2 \cdot \hat{\varphi}_1] = \Delta\rho\omega^2 l_1^\sigma(z_0)l_1^\nu(z_0) \cos \varphi.$$

Similar expressions hold for all the interaction terms.

It can be seen that the λ heterogeneity does not affect the Love waves. The reason for this is that the incoming wave (ν) enters the λ scattering term in the following way:

$$ik_\nu[\hat{\Delta}_1 \cdot \mathbf{p}^\nu(z_0, \varphi_1)] + \partial_{z_0} p_3^\nu(z_0, \varphi_1).$$

For a Love wave the polarization vector has no vertical component, and is perpendicular to the direction of propagation ($\hat{\Delta}_1$). Therefore both terms vanish if the incoming wave is a Love wave. If the outgoing wave (σ) is a Love wave the same holds, so that λ variations do not affect Love waves at all.

If the polarization vectors for Love and Rayleigh waves ((7) and (8)) are inserted in (27) then the following expression for the interaction matrix results:

$$V_{LL}^{\sigma\nu} = [l_1^\sigma l_1^\nu \Delta\rho\omega^2 - (\partial l_1^\sigma) (\partial l_1^\nu) \Delta\mu] \cos \varphi - k_\sigma k_\nu l_1^\sigma l_1^\nu \Delta\mu \cos 2\varphi \quad (29a)$$

$$V_{RL}^{\sigma\nu} = [r_1^\sigma l_1^\nu \Delta\rho\omega^2 + (k_\sigma r_2^\sigma - \partial r_1^\sigma) \partial l_1^\nu \Delta\mu] \sin \varphi - k_\sigma k_\nu r_1^\sigma l_1^\nu \Delta\mu \sin 2\varphi \quad (29b)$$

$$V_{LR}^{\sigma\nu} = -V_{RL}^{\nu\sigma} \quad (29c)$$

$$V_{RR}^{\sigma\nu} = [r_2^\sigma r_2^\nu \Delta\rho\omega^2 - (k_\sigma r_1^\sigma + \partial r_2^\sigma) (k_\nu r_1^\nu + \partial r_2^\nu) \Delta\lambda - k_\sigma k_\nu r_1^\sigma r_1^\nu \Delta\mu - 2(\partial r_2^\sigma) (\partial r_2^\nu) \Delta\mu] \\ + [r_1^\sigma r_1^\nu \Delta\rho\omega^2 - (k_\sigma r_2^\sigma - \partial r_1^\sigma) (k_\nu r_2^\nu - \partial r_1^\nu) \Delta\mu] \cos \varphi - k_\sigma k_\nu r_1^\sigma r_1^\nu \Delta\mu \cos 2\varphi. \quad (29d)$$

For convenience the z_0 dependence of the eigenfunctions is not shown explicitly. Vertical derivatives are denoted in the following abbreviated form:

$$\partial f = \frac{\partial f}{\partial z_0}(z_0).$$

Observe that the interaction terms depend in a very simple way on the scattering angle. There is no conversion from Love wave to Rayleigh wave or vice versa in the forward direction ($\varphi = 0$), or in the backward direction ($\varphi = \pi$). The interaction terms V_{RL} and V_{LR} differ only in sign, but have the same magnitude.

5 Linearized scattering with a smooth background medium

The theory of the previous sections can be generalized for a smoothly varying background medium with embedded scatterers. 'Smoothly varying' means in this context that the horizontal variations of the background medium are small on a scale of the largest horizontal wavelength under consideration. (There is of course no restriction on the vertical variations of the background medium.)

Bretherton (1968) showed that in this limit the surface wave modes decouple, and Babich *et al.* (1976) derived a ray tracing formalism for surface waves, as well as a condition for the amplitude variations along a ray. Hudson (1981) derived a parabolic approximation for surface waves, which Yomogida (1985) extended to a Gaussian beam formalism for surface waves. We shall proceed here with a derivation of the Green's function for Love waves in a smoothly varying background medium. (The derivation is completely analogous in the case of Rayleigh waves.) Since the surface wave modes are decoupled we will restrict ourselves to one mode, and modal summation is temporarily suppressed.

According to Yomogida the Love wave displacement on a ray (i.e. $n = 0$ in his notation) is in the far field:

$$\mathbf{u}^0 = \frac{\hat{\varphi}(s)\bar{l}_1(s, z)}{\sqrt{q(s)U(s)I_1(s)}} \exp[i\theta(s)]\phi_L. \quad (30)$$

In this expression \bar{l}_1 is defined by the condition $\bar{l}_1(s, 0) = 1$, $\bar{l}_1(s, z)$ is a 'local mode' since the mode varies along the ray. The phase of the Love wave is given by:

$$\theta(s) = \int_0^s \hat{k}(s') ds' \quad (31)$$

where $k(s)$ is the local wavenumber, and the integral is along the ray. The geometrical spreading factor $q(s)$ follows for a point source from the equations of dynamical ray tracing:

$$\begin{aligned} \partial_s p &= -c^{-2}(s)\partial_{nn}c(s)q \\ \partial_s q &= c(s)p, \end{aligned} \quad (32a)$$

with starting values:

$$p(0) = c^{-1}(0), \quad q(0) = 0. \quad (32b)$$

In these expressions ∂_s denotes differentiation along a ray, while ∂_n is the horizontal derivative perpendicular to a ray. Finally ϕ_L represents the excitation of the Love wave. This factor follows from the consideration that the excitation depends only on the local properties of the medium, so that ϕ_L is the same in a smoothly varying medium as in a laterally homogeneous medium with the properties of the source region. For a laterally homogeneous medium (32a, b) can be integrated to give $q(s) = s$, so that in that case:

$$u = \frac{\hat{\varphi}(s)\bar{l}_1(s, z)}{\sqrt{U(s)I_1(s)}} \cdot \frac{\exp(iks)}{\sqrt{s}} \phi_L. \quad (33)$$

A comparison with (9), (7) and the normalization condition (5) shows that ϕ_L is determined by:

$$\phi_L = \frac{\exp(i\pi/4)}{\sqrt{4\pi\omega}} l_1(z, s=0)[\hat{\varphi}(0) \cdot \mathbf{F}]. \quad (34)$$

If $l_1(z, s)$ in (30) is normalized according to (5), and (34) is used for the excitation factor, then it follows that the Love wave displacement is:

$$\mathbf{u}^0 = l_1(z, s) \hat{\varphi}(s) \frac{\exp[i(\theta(s) + \pi/4)]}{\sqrt{(\pi/2)k(s)q(s)}} l_1(z_s, s=0) [\hat{\varphi}(s=0) \cdot \mathbf{F}]. \quad (35)$$

A similar result holds for Rayleigh waves, so that the Green's function for a smoothly varying background medium has the following dyadic form:

$$G_{ij}(\mathbf{r}, \mathbf{r}_s) = p_i^\nu [z, s, \varphi(s)] \frac{\exp [i(\theta_\nu(s) + \pi/4)]}{\sqrt{(\pi/2)k_\nu(s)q_\nu(s)}} p_j^{\nu*} [z_s, s = 0, \varphi(0)]. \quad (36)$$

It should be stressed that the normalization condition (5) is crucial in obtaining the correct amplitude variations along the ray. The modal summation now includes both Love and Rayleigh waves. Note that quantities like the phase shift $\theta_\nu(s)$ or the geometrical spreading $q_\nu(s)$ are different from mode to mode. Also the ray paths are in general different for different modes, so that ray tracing has to be done for each mode separately.

The expressions for the gradient of the Green's function (10a–d) are unaffected by a smooth horizontal heterogeneity of the background medium, since the horizontal derivatives of the parameters of the medium are by assumption small compared to $k_\nu(s)$. The derivation in Sections 3 and 4 is therefore unaffected by the smooth variations in the background medium. Therefore the expression for the scattered wave is:

$$\mathbf{u}^1(\mathbf{r}) = \mathbf{p}^\sigma(z, \varphi_2(s), s) \frac{\exp [i(\theta_\sigma(s) + \pi/4)]}{\sqrt{(\pi/2)k_\sigma(s)q_\sigma(s)}} V^{\sigma\nu}(\mathbf{r}_0) \frac{\exp [i(\theta_\nu(s) + \pi/4)]}{\sqrt{(\pi/2)k_\nu(s)q_\nu(s)}} [\mathbf{p}^\nu(z_s, \varphi_1(0), 0) \cdot \mathbf{F}]. \quad (37)$$

See Fig. 3 for the definition of the variables. In principle the length along the ray path (s) depends on the mode number, but this is not shown explicitly. The interaction matrix is given by (27) or (29a–d) with the local polarization vectors. The scattering angle is now determined by the angle between the incoming and the outgoing ray at the scatterer. Therefore the scattering angle for a fixed source receiver pair is in general different for different sets of modes (σ, ν).

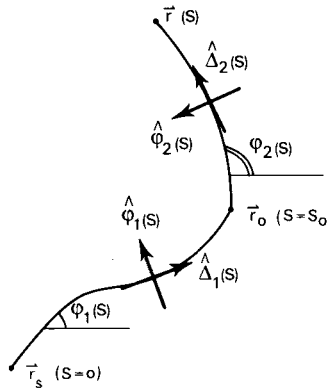


Figure 3. Geometry for the scattered wave in a smoothly varying background medium.

Note that the expression for the scattered wave depends explicitly on the scattering angle. This makes it impossible to use a Gaussian beam formalism in this context, since one has to do the ray tracing from source to scatterer to receiver in order to obtain the scattering angle. This is a time-consuming procedure since it has to be repeated for every new set of modes (σ, ν).

6 The interaction matrix for scattering by a mountain root

In the previous sections the theory of surface wave scattering was developed. The subsequent sections deal with some examples to clarify the theory. In this section the depth integrals of the interaction matrix (29a–d) are presented for the scattering of surface waves by the root of the Alps. The heterogeneity consists of a light, low velocity anomaly between 20 and 50 km, taken from Mueller & Talwani (1971). The M7 model or Nolet (1977) is used as a background medium. Both the background medium and the heterogeneity are shown in Fig. 4.

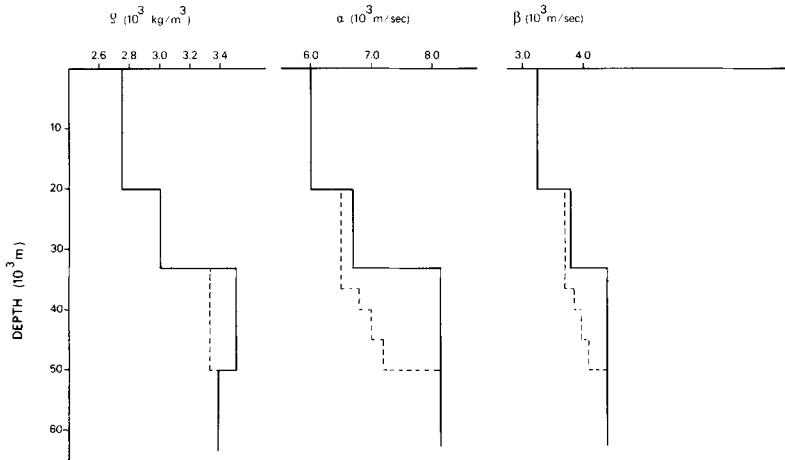


Figure 4. Density, P -wave velocity and S -wave velocity for the background medium (solid line), and the mountain root model (dashed line) used in the calculations of the interaction matrix of Section 6.

It can be seen from (29a–d) that the interaction matrix for the scattering from Rayleigh wave to Rayleigh wave, or from Love wave to Love wave has the form:

$$V_{RR \text{ or } LL} = V(0) + V(1) \cos \varphi + V(2) \cos 2\varphi.$$

Here φ is the scattering angle. In case a Rayleigh wave is converted to a Love wave, or vice versa, the interaction matrix takes the form:

$$V_{RL \text{ or } LR} = V(1) \sin \varphi + V(2) \sin 2\varphi.$$

In this section the 'sin $n\varphi$ ' scattering coefficient for the conversion of the ν th Love wave to the σ th Rayleigh wave is denoted by $V_{R\sigma \leftarrow L\nu}(n)$. A similar notation is used for the Love wave–Love wave scattering and the Rayleigh wave–Rayleigh wave scattering.

In Fig. 5 the fundamental mode interaction terms $V_{R_1 \leftarrow R_1}$, $V_{R_1 \leftarrow L_1}$ and $V_{L_1 \leftarrow L_1}$ are shown as a function of frequency. The interaction terms are given per unit area because (29a–d) has only been integrated over z . In order to obtain the strength of the scattered wave one has to multiply by the horizontal area of the scatterer. For a scatterer of 100×100 km the scattering coefficient is of order 1. However, surface waves with a period of 20 s have a wavelength of the order of 100 km, so that one cannot consider a scatterer of 100×100 km as a point scatterer. In that case one would have to integrate over the horizontal extent of the whole scatterer. In order to circumvent this complication the interaction terms are simply given per unit area.

Note that the three types of fundamental mode scattering are of the same order of magnitude. Also observe that the scattering coefficients are strongly dependent on the

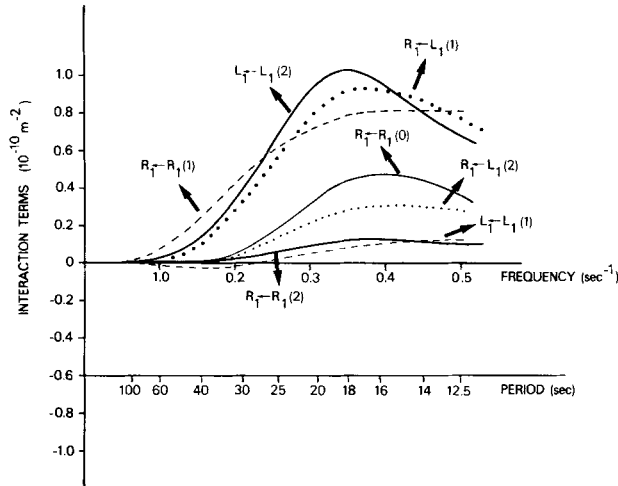


Figure 5. Fundamental mode interaction terms for different azimuth numbers for scattering by the mountain root as a function of frequency.

period. The interaction terms at 20 s are almost an order of magnitude larger than the interaction terms at 40 s. This agrees well with observations of scattered surface waves which show that 20 s Rayleigh waves are much more strongly scattered than 40 s Rayleigh waves (Levshin & Berteussen 1979). The reason for this is that for a period of 40 s the penetration depth of the surface waves is so large that the influence of the shallow scatterer on the propagation of the surface wave is relatively small. Mathematically this is realized by the normalization condition (5).

The interaction terms for $R_1 \leftarrow R_1$ scattering and $R_1 \leftarrow L_1$ conversion decreases for periods shorter than 17 s. The reason for this effect is that for these high frequencies the surface waves are too shallow to be influenced by the heterogeneity.

In order to appreciate the difference in the radiation patterns for the different fundamental mode scattering events, the scattering amplitude is shown in Fig. 6 as a function of

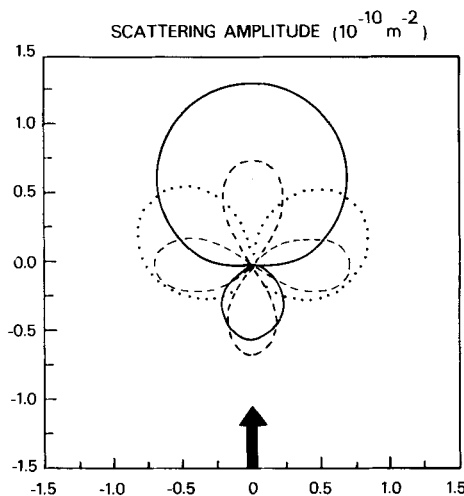


Figure 6. Radiation pattern for the scatterer of Fig. 5. The wave comes in from below. $R_1 \leftarrow R_1$ scattering is shown by a solid line, $L_1 \leftarrow L_1$ scattering by a dashed line and $R_1 \leftarrow L_1$ conversion by a dotted line.

the scattering angle for a period of 21 s. Note that there is no converted wave being radiated in the forward or in the backward direction. The $R_1 \leftarrow R_1$ scattering is much stronger in the forward direction than for backscattering, while $L_1 \leftarrow L_1$ has a much more symmetrical four lobe radiation pattern.

Fig. 5 shows that the different azimuth terms $V(n)$ in general behave in a different way as a function of frequency. Consequently, not only the strength of the radiation pattern depends on frequency, but also the shape of the radiation pattern is frequency dependent. This can be seen in Fig. 7 which shows the $R_1 \leftarrow R_1$ scattering for several periods. For a period of 40 s the scattering is very weak, and forward scattering and backscattering have almost the same strength. For larger periods the radiation pattern loses this symmetry.

For periods larger than 20 s the interaction among the fundamental modes is in general much stronger than the interactions involving higher modes. For shorter periods this does not hold any more, because for these periods the fundamental modes are too shallow to be influenced by the heterogeneity.

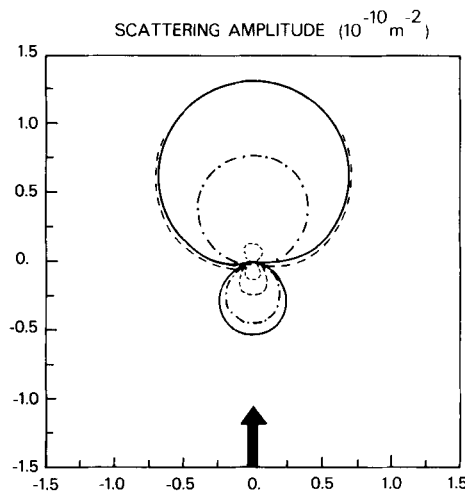


Figure 7. Radiation pattern for $R_1 \leftarrow R_1$ scattering as in Fig. 6 for different periods. The thin dashed line is for $T = 40$ s, the dashed-dotted line for $T = 26$ s, the solid line for $T = 21$ s and the thick dashed line for $T = 14$ s.

As a representative example the interaction terms $V_{R_N \leftarrow R_1}(1)$ and $V_{R_N \leftarrow R_N}(1)$ are shown in Fig. 8(a, b). Note that the coupling of the higher modes with the fundamental mode is stronger than the interaction of the higher modes with themselves. The only exception is the scattering of the first higher mode ($N = 2$) to itself for short periods. This strong scattering is caused by the fact that for periods of 10–14 s the first higher mode behaves like a Stoneley mode on the Moho, and therefore carries most of its energy at the depth of the heterogeneity.

One should be a bit careful with the conclusion that for periods larger than 20 s the higher mode scattering effects are negligible. It is true that this conclusion holds for the interaction terms $V(n)$, but it is not necessarily true for all scattering angles since for some scattering angles the fundamental mode interaction terms vanishes. As an example the Rayleigh wave radiation pattern is shown in Fig. 9 for the coupling of the fundamental mode with itself, as well as with the higher modes. The scattering amplitude for $R_1 \leftarrow R_1$ scattering vanishes for a scattering angle of 106° . This means that for this scattering angle the coupling to the higher modes dominates the $R_1 \leftarrow R_1$ scattering.

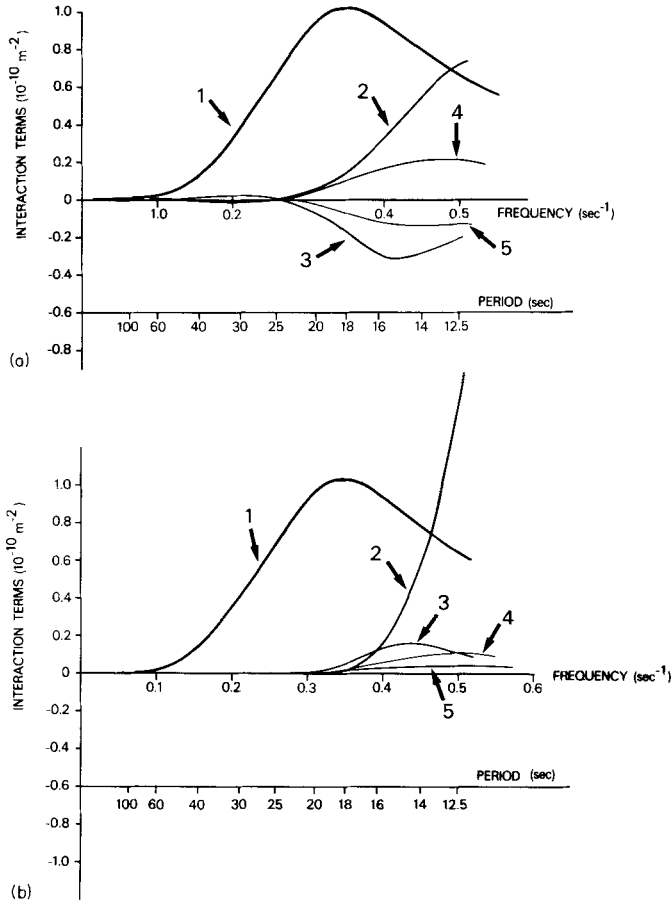


Figure 8. (a) $V_{R_N \leftarrow R_1}(1)$ interaction terms for the mountain root scatterer as a function of frequency. Numbers in figure are mode numbers N . (b) $V_{R_N \leftarrow R_N}(1)$ interaction terms for the mountain root scatterer as a function of frequency. Numbers in figure are mode numbers N .

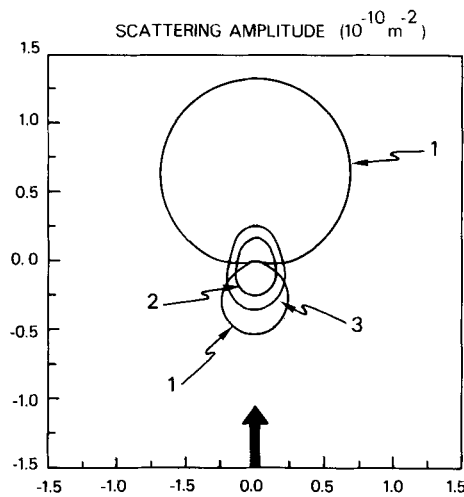


Figure 9. Radiation pattern as in Fig. 6 for $R_N \leftarrow R_1$ scattering for a period of 21 s. Numbers in the figure are mode numbers N .

7 Application of stationary phase principles to the calculation of the scattered wave

The theory presented in Sections 2–5 dealt with surface wave scattering by point scatterers. However, since the theory is linear(ized), more general inhomogeneities can be treated by integrating over the inhomogeneity. This integration can be simplified considerably by using the stationary phase approximation (Bender & Orszag 1978). Two examples are given for a laterally homogeneous background medium.

7.1 PROPAGATION THROUGH A BAND-LIKE HETEROGENEITY

Consider the propagation of surface waves through a band-like inhomogeneity confined between $x = x_L$ and $x = x_R$ (see Fig. 10). This heterogeneity is not unlike the model for the Central Graben in the North Sea, used by Kennett (1984b). The inhomogeneity is assumed to depend on y in a smooth way, compared with the horizontal wavelength of the surface waves. In that case the scattered wave is:

$$\mathbf{u}^1(\mathbf{r}_r) = \int_{x_L}^{x_R} dx \int_{-\infty}^{\infty} dy \int_0^{\infty} dz \exp [i(k_\nu X_1 + k_\sigma X_2)] \mathbf{f}_{\sigma\nu} \quad (38)$$

with

$$\mathbf{f}_{\sigma\nu} = i\mathbf{p}^\sigma(z_r, \varphi_2) \frac{V^{\sigma\nu}(x, y, z)}{\sqrt{(\pi/2)k_\sigma X_2} \sqrt{(\pi/2)k_\nu X_1}} [\mathbf{p}^\nu(z_s, \varphi_1) \cdot \mathbf{F}]. \quad (39)$$

The y integral can be evaluated with the stationary phase approximation. The point of stationarity is given by $y = 0$ for all x and z , so that the phase function can be approximated by:

$$(k_\nu X_1 + k_\sigma X_2) \approx k_\nu x + k_\sigma(x_r - x) + \frac{1}{2} \left(\frac{k_\nu}{x} + \frac{k_\sigma}{x_r - x} \right) y^2.$$

Integration over y then leads to the following approximation for the scattered wave:

$$\mathbf{u}^1(\mathbf{r}_r) \approx 2 \sqrt{\frac{2}{\pi}} \frac{\exp [i(k_\sigma x_r + 3\pi/4)]}{\sqrt{k_\nu k_\sigma}} \int_0^{\infty} dz \int_{x_L}^{x_R} dx \frac{\exp [i(k_\nu - k_\sigma)x]}{\sqrt{k_\nu(x_r - x) + k_\sigma x}} V^{\sigma\nu}(x, y = 0, z) \mathbf{p}^\sigma(z_r, \varphi_2 = 0) [\mathbf{p}^\nu(z_s, \varphi_1 = 0) \cdot \mathbf{F}]. \quad (40)$$

This means that in order to calculate the scattered wave one only needs to integrate over the line joining the source and the receiver. Equation (40) is a restatement of the ‘great circle theorem’ (Jordan 1978 or Dahlen 1979), but now in a plane geometry. The only difference is that in order to arrive at (40) we did not have to assume smoothness of the heterogeneity along the great circle, but only in the transverse direction.

Equation (40) shows that the interaction matrix is only needed for a scattering angle $\varphi = 0$. This means that mode conversions from a Love wave to a Rayleigh wave (and vice versa) vanish in this limit, since V_{RL} vanishes for $\varphi = 0$. This reflects the fact that appreciable transverse gradients of the inhomogeneity are needed to couple Love waves to Rayleigh waves.

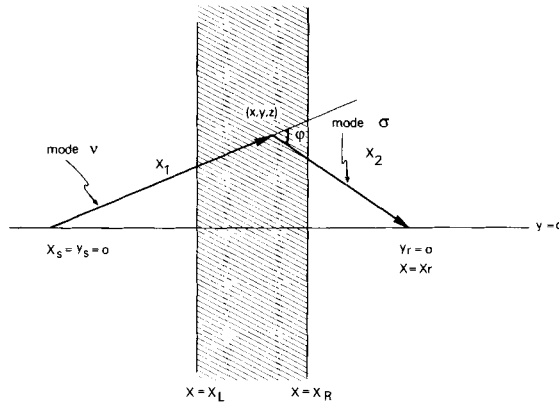


Figure 10. Geometry for surface wave scattering by a band-like heterogeneity.

For Love waves the z integral of the interaction matrix term in (40) is given by:

$$\int_0^\infty V_{LL}^{\sigma\nu}(x, y = 0, z) dz = \int_0^\infty dz [(\Delta\rho\omega^2 - k_\sigma k_\nu \Delta\mu) l_1^\sigma(z) l_1^\nu(z) - \Delta\mu (\partial_z l_1^\sigma) (\partial_z l_1^\nu)]. \quad (41)$$

This expression is the linearized form of the interaction terms (2.21) of the 2-D theory of Kennett (1984a). The only difference with Kennett's result is the appearance of the geometrical spreading factor in (40), as well as a phase shift of $\pi/4$. Both differences are caused by the fact that in this theory the surface waves are propagating in two horizontal directions.

7.2 SCATTERING BY A QUARTER-SPACE

In the previous section it was shown that only the heterogeneity on the source–receiver line influences the scattered wave if the inhomogeneity is smooth in the transverse direction. The next example shows what can happen if this condition is violated. Consider the situation shown in Fig. 11. The left half of the (x, y) plane consists of a different medium than the right half of the plane, where the source and the receiver are located. This situation models the scattering of surface waves by a sharp continental margin. The heterogeneity in the left half plane is assumed to be smooth in the horizontal direction (compared to the largest horizontal wavelength under consideration). This means that:

$$|\partial_x(\Delta\mu)| \ll |k\Delta\mu|, \quad |\partial_y(\Delta\mu)| \ll |k\Delta\mu|. \quad (42)$$

(Similar expressions hold for $\Delta\lambda$ and $\Delta\rho$.) Lastly, it is assumed that both the source and the receiver are located many wavelengths away from the continental margin.

Again, the scattered wave can be written as an integral over the inhomogeneity:

$$\mathbf{u}^1(\mathbf{r}_r) = \int_{-\infty}^\infty dx \int_{-\infty}^\infty dy \int_0^\infty dz \exp [i(k_\nu X_1 + k_\sigma X_2)] \mathbf{f}_{\sigma\nu} H(-x) \quad (43)$$

with \mathbf{f} given by (39), and H is the Heaviside function. After a partial integration in x the

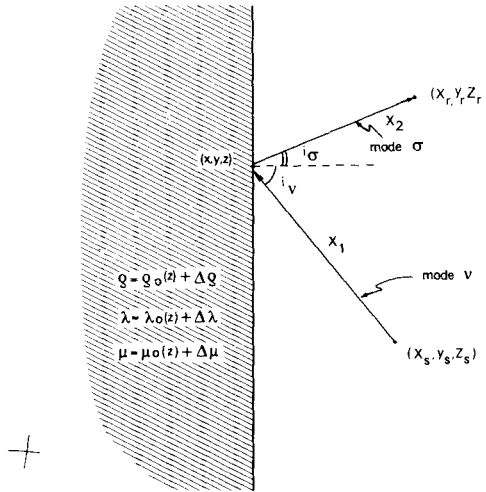


Figure 11. Geometry for surface wave scattering by a quarter-space.

scattered wave can be rewritten as:

$$u^1(r) = \int_{-\infty}^{\infty} dy \int_0^{\infty} dz \frac{\exp [i(k_\nu X_1 + k_\sigma X_2) \mathbf{f}_{\sigma\nu} H(-x)]}{i \llbracket k_\nu [(x - x_s)/X_1] + k_\sigma [(x - x_r)/X_2] \rrbracket} \Bigg|_{x=-\infty}^{x=\infty} + i \int_{-\infty}^{\infty} dx \int_{-\infty}^{\infty} dy \int_0^{\infty} dz \partial_x \left[\frac{H(-x) \mathbf{f}_{\sigma\nu}}{\llbracket k_\nu [(x - x_s)/X_1] + k_\sigma [(x - x_r)/X_2] \rrbracket} \right] \exp [i(k_\nu X_1 + k_\sigma X_2)]$$

The first term on the right side is zero if a small amount of damping is present; this can be realized by giving k_σ and k_ν a (small) positive imaginary component. The x differentiation in the second term produces three kinds of terms. Differentiation of the geometrical factors yields terms of the relative order $O(1/k_\nu X_1, 1/k_\sigma(x - x_r), \text{etc.})$ which are negligible in the far field compared to the original expression (43). The contributions of the derivatives of $\Delta\mu$, $\Delta\lambda$ and $\Delta\rho$ (which are contained in \mathbf{f}) are also negligible compared to the original expression (43) because of the smoothness we assumed (42). Therefore the dominant contribution comes from the derivative of the Heaviside function. This leads to the following expression for the scattered wave:

$$u^1(r, r) = i \int_{-\infty}^{\infty} dy \int_0^{\infty} dz \mathbf{f}_{\sigma\nu} \cdot \frac{\exp [i(k_\nu X_1 + k_\sigma X_2)]}{[k_\nu(x_s/X_1) + k_\sigma(x_r/X_2)]} \tag{44}$$

The y integral can again be evaluated with a stationary phase approximation. The phase function is:

$$\theta_{\sigma\nu}(y) = k_\nu \sqrt{x_s^2 + (y - y_s)^2} + k_\sigma \sqrt{x_r^2 + (y - y_r)^2} \tag{45}$$

Let the minimum of $\theta_{\sigma\nu}(y)$ be attained for \hat{y} , so that:

$$\theta'_{\sigma\nu}(\hat{y}) = k_\nu \frac{\hat{y} - y_s}{X_1} + k_\sigma \frac{\hat{y} - y_r}{X_2} = 0 \tag{46}$$

It then follows from a stationary phase evaluation of the y integral that the scattered wave is given by:

$$\mathbf{u}'(\mathbf{r}_r) = \sqrt{\frac{8}{\pi \theta''_{\sigma\nu}(\hat{y})}} \frac{\exp [i(k_\nu X_1 + k_\sigma X_2 + 3\pi/4)]}{[k_\nu(x_s/X_1) + k_\sigma(x_r/X_2)] \sqrt{k_\nu X_1} \sqrt{k_\sigma X_2}} \mathbf{P}^\sigma(z_r, \varphi_2) [\mathbf{P}^\nu(z_s, \varphi_1) \cdot \mathbf{F}] \Big|_{y=\hat{y}}^{x=0} \times \int_0^\infty V^{\sigma\nu}(x=0, y=\hat{y}, z) dz. \tag{47}$$

Inspection of Fig. 11 shows that the stationary phase condition (46) is just Snell's law for the reflection of surface waves:

$$\frac{\sin i_\nu}{c_\nu} = \frac{\sin i_\sigma}{c_\sigma} \quad (\text{no summation}) \tag{48}$$

where

$$c_\nu = \omega/k_\nu. \tag{49}$$

This means that for every set of modes (ν, σ) scattering by a quarter-space is equivalent to reflection by a point on the boundary between the two quarter-spaces which is determined by Snell's law. This means that the forward problem can be solved very efficiently because the cumbersome integration over the heterogeneity can be avoided. Unlike in Alsop *et al.* (1974) and Gregersen & Alsop (1974) the surface boundary condition is satisfied, since each mode satisfies the surface boundary condition. In contrast to previous studies it is not necessary to calculate the modes in both quarter-spaces in order to find the reflection coefficients.

Unfortunately, it is not possible to consider the transmission of surface waves through a continental margin by locating the receiver in the heterogeneous quarter-space. The reason for this is that in that case the far field approximation cannot be used any more.

The results derived in this section are applicable to a step-like continental margin. A smoother transition between two half-spaces can be treated numerically by dividing the transition zone into many small step discontinuities and by adding the scattered waves (47) from every step discontinuity.

8 The scattered wave in the time domain

Up to this point the theory was presented in the frequency domain. A Fourier transform makes it possible to find the scattered wave in the time domain. A stationary phase approximation of the frequency integral simplifies the final result considerably. In this section scattering by a point scatterer is discussed as an example.

The scattered wave in the time domain is given by:

$$\mathbf{u}'(\mathbf{r}_r, t) = \int_{-\infty}^\infty \mathbf{f}_{\sigma\nu}(\omega) \exp [i(k_\nu X_1 + k_\sigma X_2 - \omega t)] d\omega. \tag{50}$$

Here, \mathbf{f} is defined by (39). The frequency derivative of the phase function vanishes if the following condition is satisfied:

$$\frac{X_1}{U_\nu(\hat{\omega})} + \frac{X_2}{U_\sigma(\hat{\omega})} = t. \tag{51}$$

In this expression U_ν is the group velocity of mode ν . This condition determines a frequency $\hat{\omega}$ for every X_1 , X_2 and t . It is possible that (51) has more than one solution $\hat{\omega}$, in which case one can simply sum over the contribution of every stationary frequency. A stationary phase evaluation of the ω integral leads to the following result:

$$\mathbf{u}^1(\mathbf{r}, t) = \sqrt{\frac{8}{\pi}} \frac{1}{\sqrt{(k_\nu''(\hat{\omega})X_1 + k_\sigma''(\hat{\omega})X_2)}} \frac{\exp [i(k_\nu(\hat{\omega})X_1 + k_\sigma(\hat{\omega})X_2 - \hat{\omega}t + 3\pi/4)]}{\sqrt{k_\nu(\hat{\omega})k_\sigma(\hat{\omega})X_1X_2}} \mathbf{p}^\sigma(z, \hat{\omega}, \varphi_2) V^{\sigma\nu}(\mathbf{r}_0, \hat{\omega}) [\mathbf{p}^\nu(z_s, \hat{\omega}, \varphi_1) \cdot \mathbf{F}(\hat{\omega})]. \quad (52)$$

The prime denotes differentiation with respect to ω .

It is instructive to investigate the condition (51) in some more detail. If the modes σ and ν have the same group velocity, then (51) describes an ellipse, so that for a fixed time t all the points on the ellipse should be evaluated in (52) with the same frequency $\hat{\omega}$ (see Fig. 12a). If $U_\nu(\hat{\omega}) \neq U_\sigma(\hat{\omega})$, then (51) defines an egg-like curve and, at a given time t , all the points on the egg can be evaluated at the same frequency $\hat{\omega}$ (see Fig. 12b).

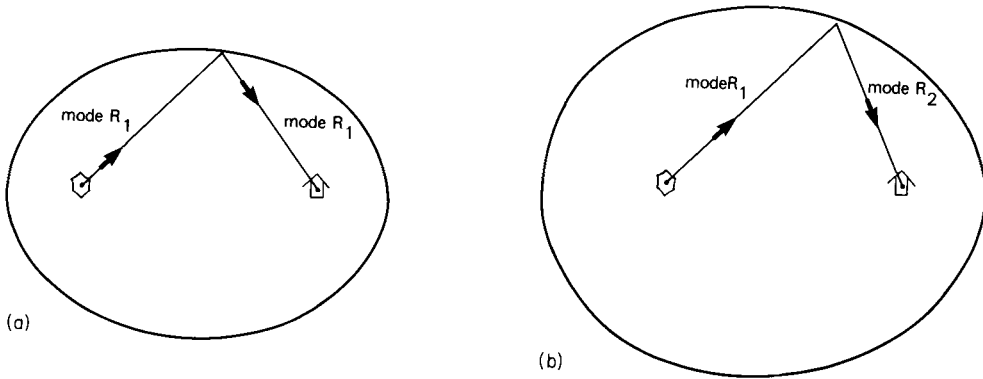


Figure 12. (a) Set of points which satisfy (51) for $R_1 \leftarrow R_1$ scattering for a period of 21 s. (b) Set of points which satisfy (51) for $R_2 \leftarrow R_1$ scattering for a period of 21 s.

9 Least squares inversion of scattered surface wave data

The theory for surface wave scattering is presented here in the Born approximation, so that there is a linear integral relation between the scattered wave (26) and the heterogeneity. (Remember that for a general configuration of scatterers (26) has to be integrated over all the scatterers, so that a r_0 integration should be performed.) This is convenient for solving the inverse problem, since the inversion of (possibly ill-posed) linear integral relations in the presence of noise is well understood. Franklin (1970) showed how to invert a discretized linear relation if the covariances of all variables are prescribed. Tarantola & Valette (1982) pointed out that discretization can be postponed to the moment of numerical implementation. The application of this formalism to the acoustic reflection problem is shown by Tarantola (1984a, b). Here a similar inversion method is presented for surface wave data. We shall assume that the source parameters and the background medium are known. If necessary these properties could be included in a simultaneous inversion with the direct wave and the scattered wave.

In the surface wave inversion problem we try to reconstruct the elastic parameters and the density from surface wave data. This means that we want to find the following model vector (which is a function of the three space variables):

$$\mathbf{m} = \begin{pmatrix} \Delta\mu \\ \Delta\lambda \\ \Delta\rho \end{pmatrix}. \tag{53}$$

The *a priori* knowledge can be incorporated by prescribing the *a priori* value of the model vector, as well as a covariance matrix. It is assumed that the *a priori* knowledge of the heterogeneity is given by:

$$\mathbf{m}_0 = 0. \tag{54}$$

The *a priori* model covariance is given by a matrix (operator) $C_m(\mathbf{r}_1, \mathbf{r}_2)$, which we shall leave unspecified. The data consist of the observations of the scattered wave, which in general consists of a superposition of different modes. It is possible that only one component of the scattered wave is measured, or that more components are measured. In general we will have data from many receivers, possibly also for different sources. We can put all these data in one data vector \mathbf{d} :

$$\mathbf{d} = \text{"}\mathbf{u}_{\text{obs}}^1\text{"}. \tag{55}$$

All the different observations are simply put below each other, so that \mathbf{d} can have any dimension. If the inversion is done in the frequency domain the scattered waves for different frequencies are all entered in the data vector (55) as separate data. Here the inversion is presented in the time domain formulation. In that case the data vector consists of the displacement measurements as a function of time, hence the data vector is a function of time. The inversion can be started once the covariance matrix of the data vector (C_d) is specified.

The inversion can be done in one step, since the theory is linear. This means that the stabilized least squares solution is given by (Tarantola 1984a):

$$\mathbf{m} = (I + C_m A^T C_d^{-1} A)^{-1} C_m A^T C_d^{-1} \mathbf{d}. \tag{56}$$

In this expression A is the gradient of the data vector in model space, i.e.

$$A = \begin{pmatrix} \frac{\partial \mathbf{u}^1}{\partial \Delta\mu} & \frac{\partial \mathbf{u}^1}{\partial \Delta\lambda} & \frac{\partial \mathbf{u}^1}{\partial \Delta\rho} \\ \vdots & \vdots & \vdots \\ \vdots & \vdots & \vdots \end{pmatrix}. \tag{57}$$

(The dots indicate that all the measured displacements are put on top of each other.) Note that A is a function of time, since \mathbf{u}^1 is a function of time.

The first step in the inversion entails weighting of the displacement components. The weighted data vector is defined by:

$$\tilde{\mathbf{u}}(t) = C_d^{-1} \mathbf{d}(t). \tag{58}$$

If one now inserts the time-dependent version of the scattered wave in (57), one obtains the following result for $A^T \tilde{u}$:

$$A^T \tilde{u}(\mathbf{r}_0) = \sum_{r,s} \int \begin{pmatrix} \frac{\partial V^{\sigma\nu}(\mathbf{r}_0)}{\partial \Delta\mu} \\ \frac{\partial V^{\sigma\nu}(\mathbf{r}_0)}{\partial \Delta\lambda} \\ \frac{\partial V^{\sigma\nu}(\mathbf{r}_0)}{\partial \Delta\rho} \end{pmatrix} g_{\sigma\nu}(\hat{\omega}, X_1, X_2) \\ [F_s(\hat{\omega}) \cdot \mathbf{p}^\nu(z_s, \hat{\omega}, \varphi_1)] \frac{\exp[-i(k_\nu(\hat{\omega})X_1 - \hat{\omega}t + 3\pi/4)]}{\sqrt{(\pi/2)k_\nu(\hat{\omega})X_1}} \frac{\exp[-ik_\sigma(\hat{\omega})X_2]}{\sqrt{(\pi/2)k_\sigma(\hat{\omega})X_2}} \\ \times [\mathbf{p}^\sigma(z_r, \hat{\omega}, \varphi_2) \cdot \tilde{u}(t)] dt \quad (59)$$

where

$$g_{\sigma\nu}(\hat{\omega}, X_1, X_2) = \sqrt{2\pi/(k_\nu''(\hat{\omega})X_1 + k_\sigma''(\hat{\omega})X_2)}. \quad (60)$$

The integration over time in (59) is performed because both A and \tilde{u} are functions of time, and a contraction over the time variable is implied by the operator product. All variables have the same meaning as in Fig. 2, for the appropriate sources and receivers. The symbol $\sum_{r,s}$ indicates that a summation over all the sources and receivers is performed. For each source–receiver pair and each value of t the value of $\hat{\omega}$ is determined by (51). If (51) has more than one solution one should sum over these solutions. The derivatives of $V^{\sigma\nu}$ can easily be obtained from (29a–d).

Just as in Tarantola (1984a) the inversion consists of a back propagation, as well as a correlation with the source function. This can be seen in (59) because this expression is the temporal correlation of a surface wave propagating back from the source to the scatterer with a surface wave propagating from the receiver to the scatterer. Equation (59) therefore implies a summation in the horizontal plane over the ellipses or egg-curves of Fig. 12. The weight factor in this summation is determined by the geometrical spreading factors, the projection of the observed scattered wave on the appropriate polarization vector, and the source characteristics.

In order to do the back propagation correctly the different modes have to be separated. In practice this is hard to realize. However, often the fundamental mode contributions are dominant, and higher mode scattering is relatively weak. Moreover, the fundamental mode wavetrain is usually separated in time from the higher mode contributions. In that case time windowing can be used to separate the fundamental modes from the higher modes, and the inversion can be done with the fundamental modes only. The fundamental Love wave and the fundamental Rayleigh wave are separated by projecting the displacement vector on the polarization vector (see (59)).

At this point only qualitative statements about the resolution can be made. The horizontal resolution and the vertical resolution are controlled by different factors. The horizontal resolution is mainly dependent on the number of sources and receivers that are available, since this determines how well the scattered wave energy can be focused on the scatterer. The vertical resolution depends mostly on the bandwidth of the signal. Synthetic

examples, or scattering data from a well-known distribution of scatterers are needed to make these statements more quantitative.

The inversion presented here can be called 'surface wave holography' because the surface waves which are scattered and reflected by the heterogeneity (the object) are projected back in space and are correlated with the source signal (the illumination) to give an image of the heterogeneity.

10 Conclusions

The scattering of surface waves has been treated in this paper in the Born approximation. This means that a linearization in the scattering effects is performed, so that the theory is only applicable for inhomogeneities which are weak enough. (See Hudson & Heritage (1982) for the validity of the Born approximation in seismic problems.) However, even if the heterogeneity is not weak, one might hope that the theory still gives a qualitative understanding of the scattering and mode conversion phenomena.

For simplicity it is assumed in this study that the surface boundary conditions are not perturbed by the heterogeneity, so that the heterogeneity is assumed to be buried. This means that this theory cannot be applied to the important case of surface wave scattering by variations in the topography without making some modifications.

The far field condition restricts the application of the theory. Because of this restriction it is impossible to consider scatterers close to the source or the receivers. This means that the theory cannot be applied if either the source or the receiver is located in a heterogeneous region. Moreover, the far field condition also makes it impossible to calculate higher order corrections to the Born approximation, since these corrections contain near field terms.

The dyadic form of the far field Green's function for either a laterally homogeneous medium or a laterally smoothly varying medium shows that the polarization vectors play a crucial role. The polarization vector determines not only the depth dependence and the displacement direction of the elastic waves; the excitation is also conveniently expressed in terms of the polarization vectors.

In the Born approximation the scattered waves are characterized by an excitation at the source, followed by an undisturbed propagation to the scatterer. Here scattering and mode conversion occur. These effects are described by the interaction matrix. After the scattering an undisturbed propagation to the receiver occurs. The 'undisturbed propagation' can be either in a laterally homogeneous medium, or in a laterally smoothly varying background medium.

Stationary phase theorems are very useful in simplifying the resulting integrals over the heterogeneity. It is shown that if the inhomogeneity is smooth in the transverse direction, then only the heterogeneity on the source-receiver line influences the scattered wave. This is the analogy of the 'great circle theorem' in a plane geometry.

The same principle holds for scattering by a quarter-space. It is shown that in the far field limit for each pair of incoming and outgoing modes the scattering is determined by a reflection point on the interface between the two quarter-spaces. The phase speeds of the incoming and the reflected surface wave determine this point by means of Snell's law.

The linearized scattering theory can be used in conjunction with the inversion algorithm of Tarantola (1984a). The inversion is formulated in a way which is reminiscent of holography techniques used in optics. This kind of inversion will be tested with data from the NARS array (Nolet & Vlaar 1982 and Dost, Van Wettum & Nolet 1984), but only a limited resolution can be expected with a small number of stations and a few source positions. A

dense network, as is presented in the PASSCAL proposal (1984), would be ideal for an accurate reconstruction of lateral heterogeneities with surface wave holography.

Acknowledgment

I thank Guust Nolet not only for his help and advice, but most importantly for creating a stimulating environment for doing seismological research.

References

- Aki, K. & Richards, P. G., 1980. *Quantitative Seismology*, volume 1, Freeman, San Francisco.
- Alsop, L. E., 1966. Transmission and reflection of Love waves at a vertical discontinuity, *J. geophys. Res.*, **71**, 3969–3984.
- Alsop, L. E., Goodman, A. S. & Gregersen, S., 1974. Reflection and transmission of inhomogeneous waves with particular application to Rayleigh waves, *Bull. seism. Soc. Am.*, **64**, 1635–1652.
- Babich, V. M., Chikhachev, B. A. & Yanovskaya, T. B., 1976. Surface waves in a vertically inhomogeneous elastic halfspace with a weak horizontal inhomogeneity, *Izv Phys. Earth*, **12**, 242–245.
- Backus, G. E., 1964. Geographical interpretation of measurements of average phase velocities of surface waves over great circular and great semi circular paths, *Bull. seism. Soc. Am.*, **54**, 571–610.
- Bender, C. M. & Orszag, S. A., 1978. *Advanced Mathematical Methods for Scientists and Engineers*, McGraw-Hill, New York.
- Ben-Menahem, A. & Singh, S. J., 1968. Eigenvector dyads with application to geophysical theory, *Geophys. J. R. astr. Soc.*, **16**, 417–452.
- Bretherton, F. P., 1968. Propagation in slowly varying waveguides, *Proc. R. Soc., A*, **302**, 555–576.
- Bungum, H. & Capon, J., 1974. Coda pattern and multipathing propagation of Raleigh waves at NORSAR, *Phys. Earth planet. Int.*, **9**, 111–127.
- Dahlen, F. A., 1979. The spectra of unresolved split normal mode multiplets, *Geophys. J. R. astr. Soc.*, **58**, 1–33.
- Dost, B., Van Wettum, A. & Nolet, G., 1984. The NARS array, *Geologie Mijnb.*, **63**, 381–386.
- Franklin, J. N., 1970. Well posed stochastic extensions of ill-posed linear problems, *J. Math. Analysis Applic.*, **31**, 682–716.
- Gregersen, S. & Alsop, L. E., 1974. Amplitudes of horizontally refracted Love waves, *Bull. seism. Soc. Am.*, **64**, 535–553.
- Harvey, D. J., 1981. Seismogram synthesis using normal mode superposition: the locked mode approximation, *Geophys. J. R. astr. Soc.*, **66**, 37–70.
- Herrera, I., 1964. A perturbation method for elastic wave propagation, *J. geophys. Res.*, **69**, 3845–3851.
- Herrera, I. & Mal, A. K., 1965. A perturbation method for elastic wave propagation 2. Small inhomogeneities, *J. geophys. Res.*, **70**, 871–883.
- Hudson, J. A., 1977a. The passage of elastic waves through an anomalous region – IV. Transmission of Love waves through a laterally varying structure, *Geophys. J. R. astr. Soc.*, **49**, 645–654.
- Hudson, J. A., 1977b. Scattered waves in the coda of *P*, *J. Geophys.*, **43**, 359–374.
- Hudson, J. A., 1981. A parabolic approximation for surface waves, *Geophys. J. R. astr. Soc.*, **67**, 755–770.
- Hudson, J. A. & Heritage, J. R., 1982. The use of the Born approximation in seismic scattering problems, *Geophys. J. R. astr. Soc.*, **66**, 221–240.
- Its, E. & Yanovskaya, T. B., 1985. Propagation of surface waves in a half space with vertical, inclined or curved interfaces, *Wave Motion*, **7**, 79–94.
- Jordan, T. H., 1978. A procedure for estimating lateral variations from low frequency eigenspectra data, *Geophys. J. R. astr. Soc.*, **52**, 441–455.
- Kennett, B. L. N., 1972. Seismic waves in laterally inhomogeneous media, *Geophys. J. R. astr. Soc.*, **27**, 301–325.
- Kennett, B. L. N., 1984a. Guided wave propagation in laterally varying media – I. Theoretical development, *Geophys. J. R. astr. Soc.*, **79**, 235–255.
- Kennett, B. L. N., 1984b. Guided wave propagation in laterally varying media – II. *L_g* waves in north-western Europe, *Geophys. J. R. astr. Soc.*, **79**, 256–267.
- Knopoff, L. & Hudson, J. A., 1964. Transmission for Love waves past a continental margin, *J. geophys. Res.*, **69**, 1649–1653.

- Levshin, A. & Berteussen, K. A., 1979. Anomalous propagation of surface waves in the Barentz Sea as inferred from NORSAR recordings, *Geophys. J. R. astr. Soc.*, **56**, 97–118.
- Malichewsky, P., 1979. Eine Verbesserung von Alsops Methode zur Bestimmung der Reflexions- und Transmissionskoeffizienten von Oberflächwellen, *Pure appl. Geophys.*, **117**, 1045–1049.
- Malin, P. E., 1980. A first order scattering solution for modelling elastic wave codas – I. The acoustic case, *Geophys. J. R. astr. Soc.*, **63**, 361–380.
- Malin, P. E. & Phinney, R. A., 1985. On the relative scattering of *P*- and *S*-waves, *Geophys. J. R. astr. Soc.*, **80**, 603–618.
- Mueller, S. & Talwani, M., 1971. A crustal section across the Eastern Alps based on gravity and seismic refraction data, *Pure appl. Geophys.*, **85**, 226.
- Nolet, G., 1977. The upper mantle under Western Europe inferred from the dispersion of Raleigh modes, *J. Geophys.*, **43**, 265–285.
- Nolet, G. & Vlaar, N. J., 1982. The NARS project: probing the Earth's interior with a large seismic antenna, *Terra Cognita*, **2**, 17–25.
- PASSCAL, 1984. Program for Array Seismic Studies of the Continental Lithosphere, issued by the Incorporated Research Institute for Seismology.
- Tarantola, A., 1984a. Inversion of seismic reflection data in the acoustic approximation, *Geophysics*, **49**, 1259–1266.
- Tarantola, A., 1984b. Linearized inversion of seismic reflection data, *Geophys. Prospect.*, **32**, 998–1015.
- Tarantola, A. & Valette, B., 1982. Generalized nonlinear inverse problems solved using the least squares criterion, *Rev. Geophys. Space Phys.*, **20**, 219–232.
- Wu, R. & Aki, K., 1985. Scattering characteristics of elastic waves by an elastic heterogeneity, *Geophysics*, **50**, 582–595.
- Yomogida, K., 1985. Gaussian beams for surface waves in laterally slowly-varying media, *Geophys. J. R. astr. Soc.*, **82**, 511–534.
- Yomogida, K. & Aki, K., 1985. Total waveform synthesis of surface waves in laterally heterogeneous earth by Gaussian beam method, *J. geophys. Res.*, **90**, 7665–7688.